

Search for a Higgs boson produced in association with a Z boson in $p\bar{p}$ collisions

V.M. Abazov,³⁵ B. Abbott,⁷⁵ M. Abolins,⁶⁵ B.S. Acharya,²⁸ M. Adams,⁵¹ T. Adams,⁴⁹ E. Aguilo,⁵ S.H. Ahn,³⁰ M. Ahsan,⁵⁹ G.D. Alexeev,³⁵ G. Alkhazov,³⁹ A. Alton,^{64,*} G. Alverson,⁶³ G.A. Alves,² M. Anastasoaie,³⁴ L.S. Ancu,³⁴ T. Andeen,⁵³ S. Anderson,⁴⁵ B. Andrieu,¹⁶ M.S. Anzelc,⁵³ Y. Arnoud,¹³ M. Arov,⁶⁰ M. Arthaud,¹⁷ A. Askew,⁴⁹ B. Åsman,⁴⁰ A.C.S. Assis Jesus,³ O. Atramentov,⁴⁹ C. Autermann,²⁰ C. Avila,⁷ C. Ay,²³ F. Badaud,¹² A. Baden,⁶¹ L. Bagby,⁵² B. Baldin,⁵⁰ D.V. Bandurin,⁵⁹ P. Banerjee,²⁸ S. Banerjee,²⁸ E. Barberis,⁶³ A.-F. Barfuss,¹⁴ P. Bargassa,⁸⁰ P. Baringer,⁵⁸ J. Barreto,² J.F. Bartlett,⁵⁰ U. Bassler,¹⁶ D. Bauer,⁴³ S. Beale,⁵ A. Bean,⁵⁸ M. Begalli,³ M. Begel,⁷¹ C. Belanger-Champagne,⁴⁰ L. Bellantoni,⁵⁰ A. Bellavance,⁵⁰ J.A. Benitez,⁶⁵ S.B. Beri,²⁶ G. Bernardi,¹⁶ R. Bernhard,²² L. Berntzon,¹⁴ I. Bertram,⁴² M. Besançon,¹⁷ R. Beuselinck,⁴³ V.A. Bezzubov,³⁸ P.C. Bhat,⁵⁰ V. Bhatnagar,²⁶ C. Biscarat,¹⁹ G. Blazey,⁵² F. Blekman,⁴³ S. Blessing,⁴⁹ D. Bloch,¹⁸ K. Bloom,⁶⁷ A. Boehlein,⁵⁰ D. Boline,⁶² T.A. Bolton,⁵⁹ G. Borissov,⁴² K. Bos,³³ T. Bose,⁷⁷ A. Brandt,⁷⁸ R. Brock,⁶⁵ G. Brooijmans,⁷⁰ A. Bross,⁵⁰ D. Brown,⁷⁸ N.J. Buchanan,⁴⁹ D. Buchholz,⁵³ M. Buehler,⁸¹ V. Buescher,²¹ S. Burdin,⁴² S. Burke,⁴⁵ T.H. Burnett,⁸² C.P. Buszello,⁴³ J.M. Butler,⁶² P. Calfayan,²⁴ S. Calvet,¹⁴ J. Cammin,⁷¹ S. Caron,³³ W. Carvalho,³ B.C.K. Casey,⁷⁷ N.M. Cason,⁵⁵ H. Castilla-Valdez,³² S. Chakrabarti,¹⁷ D. Chakraborty,⁵² K. Chan,⁵ K.M. Chan,⁵⁵ A. Chandra,⁴⁸ F. Charles,¹⁸ E. Cheu,⁴⁵ F. Chevallier,¹³ D.K. Cho,⁶² S. Choi,³¹ B. Choudhary,²⁷ L. Christofek,⁷⁷ T. Christoudias,⁴³ S. Cihangir,⁵⁰ D. Claes,⁶⁷ B. Clément,¹⁸ C. Clément,⁴⁰ Y. Coadou,⁵ M. Cooke,⁸⁰ W.E. Cooper,⁵⁰ M. Corcoran,⁸⁰ F. Couderc,¹⁷ M.-C. Cousinou,¹⁴ S. Crépé-Renaudin,¹³ D. Cutts,⁷⁷ M. Ćwiok,²⁹ H. da Motta,² A. Das,⁶² G. Davies,⁴³ K. De,⁷⁸ P. de Jong,³³ S.J. de Jong,³⁴ E. De La Cruz-Burelo,⁶⁴ C. De Oliveira Martins,³ J.D. Degenhardt,⁶⁴ F. Déliot,¹⁷ M. Demarteau,⁵⁰ R. Demina,⁷¹ D. Denisov,⁵⁰ S.P. Denisov,³⁸ S. Desai,⁵⁰ H.T. Diehl,⁵⁰ M. Diesburg,⁵⁰ A. Dominguez,⁶⁷ H. Dong,⁷² L.V. Dudko,³⁷ L. Duflot,¹⁵ S.R. Dugad,²⁸ D. Duggan,⁴⁹ A. Duperrin,¹⁴ J. Dyer,⁶⁵ A. Dyshkant,⁵² M. Eads,⁶⁷ D. Edmunds,⁶⁵ J. Ellison,⁴⁸ V.D. Elvira,⁵⁰ Y. Enari,⁷⁷ S. Eno,⁶¹ P. Ermolov,³⁷ H. Evans,⁵⁴ A. Evdokimov,⁷³ V.N. Evdokimov,³⁸ A.V. Ferapontov,⁵⁹ T. Ferbel,⁷¹ F. Fiedler,²⁴ F. Filthaut,³⁴ W. Fisher,⁵⁰ H.E. Fisk,⁵⁰ M. Ford,⁴⁴ M. Fortner,⁵² H. Fox,²² S. Fu,⁵⁰ S. Fuess,⁵⁰ T. Gadfort,⁸² C.F. Galea,³⁴ E. Gallas,⁵⁰ E. Galyaev,⁵⁵ C. Garcia,⁷¹ A. Garcia-Bellido,⁸² V. Gavrilov,³⁶ P. Gay,¹² W. Geist,¹⁸ D. Gelé,¹⁸ C.E. Gerber,⁵¹ Y. Gershtein,⁴⁹ D. Gillberg,⁵ G. Ginther,⁷¹ N. Gollub,⁴⁰ B. Gómez,⁷ A. Goussiou,⁵⁵ P.D. Grannis,⁷² H. Greenlee,⁵⁰ Z.D. Greenwood,⁶⁰ E.M. Gregores,⁴ G. Grenier,¹⁹ Ph. Gris,¹² J.-F. Grivaz,¹⁵ A. Grohsjean,²⁴ S. Grünendahl,⁵⁰ M.W. Grünewald,²⁹ F. Guo,⁷² J. Guo,⁷² G. Gutierrez,⁵⁰ P. Gutierrez,⁷⁵ A. Haas,⁷⁰ N.J. Hadley,⁶¹ P. Haefner,²⁴ S. Hagopian,⁴⁹ J. Haley,⁶⁸ I. Hall,⁷⁵ R.E. Hall,⁴⁷ L. Han,⁶ K. Hanagaki,⁵⁰ P. Hansson,⁴⁰ K. Harder,⁴⁴ A. Harel,⁷¹ R. Harrington,⁶³ J.M. Hauptman,⁵⁷ R. Hauser,⁶⁵ J. Hays,⁴³ T. Hebbeker,²⁰ D. Hedin,⁵² J.G. Hegeman,³³ J.M. Heinmiller,⁵¹ A.P. Heinson,⁴⁸ U. Heintz,⁶² C. Hensel,⁵⁸ K. Herner,⁷² G. Hesketh,⁶³ M.D. Hildreth,⁵⁵ R. Hirosky,⁸¹ J.D. Hobbs,⁷² B. Hoeneisen,¹¹ H. Hoeth,²⁵ M. Hohlfeld,²¹ S.J. Hong,³⁰ R. Hooper,⁷⁷ S. Hossain,⁷⁵ P. Houben,³³ Y. Hu,⁷² Z. Hubacek,⁹ V. Hynek,⁸ I. Iashvili,⁶⁹ R. Illingworth,⁵⁰ A.S. Ito,⁵⁰ S. Jabeen,⁶² M. Jaffré,¹⁵ S. Jain,⁷⁵ K. Jakobs,²² C. Jarvis,⁶¹ R. Jesik,⁴³ K. Johns,⁴⁵ C. Johnson,⁷⁰ M. Johnson,⁵⁰ A. Jonckheere,⁵⁰ P. Jonsson,⁴³ A. Juste,⁵⁰ D. Käfer,²⁰ S. Kahn,⁷³ E. Kajfasz,¹⁴ A.M. Kalinin,³⁵ J.M. Kalk,⁶⁰ J.R. Kalk,⁶⁵ S. Kappler,²⁰ D. Karmanov,³⁷ J. Kasper,⁶² P. Kasper,⁵⁰ I. Katsanos,⁷⁰ D. Kau,⁴⁹ R. Kaur,²⁶ V. Kaushik,⁷⁸ R. Kehoe,⁷⁹ S. Kermiche,¹⁴ N. Khalatyan,³⁸ A. Khanov,⁷⁶ A. Kharchilava,⁶⁹ Y.M. Kharzeev,³⁵ D. Khatidze,⁷⁰ H. Kim,³¹ T.J. Kim,³⁰ M.H. Kirby,³⁴ M. Kirsch,²⁰ B. Klíma,⁵⁰ J.M. Kohli,²⁶ J.-P. Konrath,²² M. Kopal,⁷⁵ V.M. Korablev,³⁸ B. Kothari,⁷⁰ A.V. Kozelov,³⁸ D. Krop,⁵⁴ A. Kryemadhi,⁸¹ T. Kuhl,²³ A. Kumar,⁶⁹ S. Kunori,⁶¹ A. Kupco,¹⁰ T. Kurča,¹⁹ J. Kvita,⁸ D. Lam,⁵⁵ S. Lammers,⁷⁰ G. Landsberg,⁷⁷ J. Lazoflores,⁴⁹ P. Lebrun,¹⁹ W.M. Lee,⁵⁰ A. Leflat,³⁷ F. Lehner,⁴¹ J. Lellouch,¹⁶ V. Lesne,¹² J. Leveque,⁴⁵ P. Lewis,⁴³ J. Li,⁷⁸ L. Li,⁴⁸ Q.Z. Li,⁵⁰ S.M. Lietti,⁴ J.G.R. Lima,⁵² D. Lincoln,⁵⁰ J. Linnemann,⁶⁵ V.V. Lipaev,³⁸ R. Lipton,⁵⁰ Y. Liu,⁶ Z. Liu,⁵ L. Lobo,⁴³ A. Lobodenko,³⁹ M. Lokajicek,¹⁰ A. Lounis,¹⁸ P. Love,⁴² H.J. Lubatti,⁸² A.L. Lyon,⁵⁰ A.K.A. Maciel,² D. Mackin,⁸⁰ R.J. Madaras,⁴⁶ P. Mättig,²⁵ C. Magass,²⁰ A. Magerkurth,⁶⁴ N. Makovec,¹⁵ P.K. Mal,⁵⁵ H.B. Malbouisson,³ S. Malik,⁶⁷ V.L. Malyshev,³⁵ H.S. Mao,⁵⁰ Y. Maravin,⁵⁹ B. Martin,¹³ R. McCarthy,⁷² A. Melnitchouk,⁶⁶ A. Mendes,¹⁴ L. Mendoza,⁷ P.G. Mercadante,⁴ M. Merkin,³⁷ K.W. Merritt,⁵⁰ A. Meyer,²⁰ J. Meyer,²¹ M. Michaut,¹⁷ T. Millet,¹⁹ J. Mitrevski,⁷⁰ J. Molina,³ R.K. Mommsen,⁴⁴ N.K. Mondal,²⁸ R.W. Moore,⁵ T. Moulik,⁵⁸ G.S. Muanza,¹⁹ M. Mulders,⁵⁰ M. Mulhearn,⁷⁰ O. Mundal,²¹ L. Mundim,³ E. Nagy,¹⁴ M. Naimuddin,⁵⁰ M. Narain,⁷⁷ N.A. Naumann,³⁴ H.A. Neal,⁶⁴ J.P. Negret,⁷ P. Neustroev,³⁹ H. Nilsen,²²

C. Noeding,²² A. Nomerotski,⁵⁰ S.F. Novaes,⁴ T. Nunnemann,²⁴ V. O'Dell,⁵⁰ D.C. O'Neil,⁵ G. Obrant,³⁹ C. Ochando,¹⁵ D. Onoprienko,⁵⁹ N. Oshima,⁵⁰ J. Osta,⁵⁵ R. Otec,⁹ G.J. Otero y Garzón,⁵¹ M. Owen,⁴⁴ P. Padley,⁸⁰ M. Pangilinan,⁷⁷ N. Parashar,⁵⁶ S.-J. Park,⁷¹ S.K. Park,³⁰ J. Parsons,⁷⁰ R. Partridge,⁷⁷ N. Parua,⁵⁴ A. Patwa,⁷³ G. Pawloski,⁸⁰ P.M. Perea,⁴⁸ K. Peters,⁴⁴ Y. Peters,²⁵ P. Pétroff,¹⁵ M. Petteni,⁴³ R. Piegaia,¹ J. Piper,⁶⁵ M.-A. Pleier,²¹ P.L.M. Podesta-Lerma,^{32,§} V.M. Podstavkov,⁵⁰ Y. Pogorelov,⁵⁵ M.-E. Pol,² A. Pompos,⁷⁵ B.G. Pope,⁶⁵ A.V. Popov,³⁸ C. Potter,⁵ W.L. Prado da Silva,³ H.B. Prosper,⁴⁹ S. Protopopescu,⁷³ J. Qian,⁶⁴ A. Quadt,²¹ B. Quinn,⁶⁶ A. Rakitine,⁴² M.S. Rangel,² K.J. Rani,²⁸ K. Ranjan,²⁷ P.N. Ratoff,⁴² P. Renkel,⁷⁹ S. Reucroft,⁶³ P. Rich,⁴⁴ M. Rijssenbeek,⁷² I. Ripp-Baudot,¹⁸ F. Rizatdinova,⁷⁶ S. Robinson,⁴³ R.F. Rodrigues,³ C. Royon,¹⁷ P. Rubinov,⁵⁰ R. Ruchti,⁵⁵ G. Safronov,³⁶ G. Sajot,¹³ A. Sánchez-Hernández,³² M.P. Sanders,¹⁶ A. Santoro,³ G. Savage,⁵⁰ L. Sawyer,⁶⁰ T. Scanlon,⁴³ D. Schaile,²⁴ R.D. Schamberger,⁷² Y. Scheglov,³⁹ H. Schellman,⁵³ P. Schieferdecker,²⁴ T. Schliephake,²⁵ C. Schmitt,²⁵ C. Schwanenberger,⁴⁴ A. Schwartzman,⁶⁸ R. Schwienhorst,⁶⁵ J. Sekaric,⁴⁹ S. Sengupta,⁴⁹ H. Severini,⁷⁵ E. Shabalina,⁵¹ M. Shamim,⁵⁹ V. Shary,¹⁷ A.A. Shchukin,³⁸ R.K. Shivpuri,²⁷ D. Shpakov,⁵⁰ V. Siccardi,¹⁸ V. Simak,⁹ V. Sirotenko,⁵⁰ P. Skubic,⁷⁵ P. Slattery,⁷¹ D. Smirnov,⁵⁵ R.P. Smith,⁵⁰ G.R. Snow,⁶⁷ J. Snow,⁷⁴ S. Snyder,⁷³ S. Söldner-Rembold,⁴⁴ L. Sonnenschein,¹⁶ A. Sopczak,⁴² M. Sosebee,⁷⁸ K. Soustruznik,⁸ M. Souza,² B. Spurlock,⁷⁸ J. Stark,¹³ J. Steele,⁶⁰ V. Stolin,³⁶ A. Stone,⁵¹ D.A. Stoyanova,³⁸ J. Strandberg,⁶⁴ S. Strandberg,⁴⁰ M.A. Strang,⁶⁹ M. Strauss,⁷⁵ R. Ströhmer,²⁴ D. Strom,⁵³ M. Strovink,⁴⁶ L. Stutte,⁵⁰ S. Sumowidagdo,⁴⁹ P. Svoisky,⁵⁵ A. Szajdor,³ M. Talby,¹⁴ P. Tamburello,⁴⁵ A. Tanasijczuk,¹ W. Taylor,⁵ P. Telford,⁴⁴ J. Temple,⁴⁵ B. Tiller,²⁴ F. Tissandier,¹² M. Titov,¹⁷ V.V. Tokmenin,³⁵ M. Tomoto,⁵⁰ T. Toole,⁶¹ I. Torchiani,²² T. Trefzger,²³ D. Tsybychev,⁷² B. Tuchming,¹⁷ C. Tully,⁶⁸ P.M. Tuts,⁷⁰ R. Unalan,⁶⁵ L. Uvarov,³⁹ S. Uvarov,³⁹ S. Uzunyan,⁵² B. Vachon,⁵ P.J. van den Berg,³³ B. van Eijk,³⁵ R. Van Kooten,⁵⁴ W.M. van Leeuwen,³³ N. Varelas,⁵¹ E.W. Varnes,⁴⁵ A. Vartapetian,⁷⁸ I.A. Vasilyev,³⁸ M. Vaupel,²⁵ P. Verdier,¹⁹ L.S. Vertogradov,³⁵ M. Verzocchi,⁵⁰ F. Villeneuve-Seguier,⁴³ P. Vint,⁴³ E. Von Toerne,⁵⁹ M. Voutilainen,^{67,‡} M. Vreeswijk,³³ R. Wagner,⁶⁸ H.D. Wahl,⁴⁹ L. Wang,⁶¹ M.H.L.S Wang,⁵⁰ J. Warchol,⁵⁵ G. Watts,⁸² M. Wayne,⁵⁵ G. Weber,²³ M. Weber,⁵⁰ H. Weerts,⁶⁵ A. Wenger,^{22,#} N. Wermes,²¹ M. Wetstein,⁶¹ A. White,⁷⁸ D. Wicke,²⁵ G.W. Wilson,⁵⁸ S.J. Wimpenny,⁴⁸ M. Wobisch,⁶⁰ D.R. Wood,⁶³ T.R. Wyatt,⁴⁴ Y. Xie,⁷⁷ S. Yacoob,⁵³ R. Yamada,⁵⁰ M. Yan,⁶¹ T. Yasuda,⁵⁰ Y.A. Yatsunenko,³⁵ K. Yip,⁷³ H.D. Yoo,⁷⁷ S.W. Youn,⁵³ C. Yu,¹³ J. Yu,⁷⁸ A. Yurkewicz,⁷² A. Zatserklyaniy,⁵² C. Zeitnitz,²⁵ D. Zhang,⁵⁰ T. Zhao,⁸² B. Zhou,⁶⁴ J. Zhu,⁷² M. Zielinski,⁷¹ D. Ziemińska,⁵⁴ A. Ziemiński,⁵⁴ L. Zivkovic,⁷⁰ V. Zutshi,⁵² and E.G. Zverev³⁷ (DØ Collaboration)

¹Universidad de Buenos Aires, Buenos Aires, Argentina

²LAFEX, Centro Brasileiro de Pesquisas Físicas, Rio de Janeiro, Brazil

³Universidade do Estado do Rio de Janeiro, Rio de Janeiro, Brazil

⁴Instituto de Física Teórica, Universidade Estadual Paulista, São Paulo, Brazil

⁵University of Alberta, Edmonton, Alberta, Canada, Simon Fraser University, Burnaby, British Columbia, Canada, York University, Toronto, Ontario, Canada, and McGill University, Montreal, Quebec, Canada

⁶University of Science and Technology of China, Hefei, People's Republic of China

⁷Universidad de los Andes, Bogotá, Colombia

⁸Center for Particle Physics, Charles University, Prague, Czech Republic

⁹Czech Technical University, Prague, Czech Republic

¹⁰Center for Particle Physics, Institute of Physics, Academy of Sciences of the Czech Republic, Prague, Czech Republic

¹¹Universidad San Francisco de Quito, Quito, Ecuador

¹²Laboratoire de Physique Corpusculaire, IN2P3-CNRS, Université Blaise Pascal, Clermont-Ferrand, France

¹³Laboratoire de Physique Subatomique et de Cosmologie, IN2P3-CNRS, Université de Grenoble 1, Grenoble, France

¹⁴CPPM, IN2P3-CNRS, Université de la Méditerranée, Marseille, France

¹⁵Laboratoire de l'Accélérateur Linéaire, IN2P3-CNRS et Université Paris-Sud, Orsay, France

¹⁶LPNHE, IN2P3-CNRS, Universités Paris VI and VII, Paris, France

¹⁷DAPNIA/Service de Physique des Particules, CEA, Saclay, France

¹⁸IPHC, Université Louis Pasteur et Université de Haute Alsace, CNRS, IN2P3, Strasbourg, France

¹⁹IPNL, Université Lyon 1, CNRS/IN2P3, Villeurbanne, France and Université de Lyon, Lyon, France

²⁰III. Physikalischess Institut A, RWTH Aachen, Aachen, Germany

²¹Physikalisches Institut, Universität Bonn, Bonn, Germany

²²Physikalisches Institut, Universität Freiburg, Freiburg, Germany

²³Institut für Physik, Universität Mainz, Mainz, Germany

²⁴Ludwig-Maximilians-Universität München, München, Germany

²⁵Fachbereich Physik, University of Wuppertal, Wuppertal, Germany

²⁶Panjab University, Chandigarh, India

²⁷Delhi University, Delhi, India

- ²⁸*Tata Institute of Fundamental Research, Mumbai, India*
²⁹*University College Dublin, Dublin, Ireland*
³⁰*Korea Detector Laboratory, Korea University, Seoul, Korea*
³¹*SungKyunKwan University, Suwon, Korea*
³²*CINVESTAV, Mexico City, Mexico*
- ³³*FOM-Institute NIKHEF and University of Amsterdam/NIKHEF, Amsterdam, The Netherlands*
³⁴*Radboud University Nijmegen/NIKHEF, Nijmegen, The Netherlands*
³⁵*Joint Institute for Nuclear Research, Dubna, Russia*
³⁶*Institute for Theoretical and Experimental Physics, Moscow, Russia*
³⁷*Moscow State University, Moscow, Russia*
³⁸*Institute for High Energy Physics, Protvino, Russia*
³⁹*Petersburg Nuclear Physics Institute, St. Petersburg, Russia*
- ⁴⁰*Lund University, Lund, Sweden, Royal Institute of Technology and Stockholm University, Stockholm, Sweden, and Uppsala University, Uppsala, Sweden*
- ⁴¹*Physik Institut der Universität Zürich, Zürich, Switzerland*
⁴²*Lancaster University, Lancaster, United Kingdom*
⁴³*Imperial College, London, United Kingdom*
⁴⁴*University of Manchester, Manchester, United Kingdom*
⁴⁵*University of Arizona, Tucson, Arizona 85721, USA*
- ⁴⁶*Lawrence Berkeley National Laboratory and University of California, Berkeley, California 94720, USA*
⁴⁷*California State University, Fresno, California 93740, USA*
⁴⁸*University of California, Riverside, California 92521, USA*
⁴⁹*Florida State University, Tallahassee, Florida 32306, USA*
- ⁵⁰*Fermi National Accelerator Laboratory, Batavia, Illinois 60510, USA*
⁵¹*University of Illinois at Chicago, Chicago, Illinois 60607, USA*
⁵²*Northern Illinois University, DeKalb, Illinois 60115, USA*
⁵³*Northwestern University, Evanston, Illinois 60208, USA*
⁵⁴*Indiana University, Bloomington, Indiana 47405, USA*
⁵⁵*University of Notre Dame, Notre Dame, Indiana 46556, USA*
⁵⁶*Purdue University Calumet, Hammond, Indiana 46323, USA*
⁵⁷*Iowa State University, Ames, Iowa 50011, USA*
⁵⁸*University of Kansas, Lawrence, Kansas 66045, USA*
⁵⁹*Kansas State University, Manhattan, Kansas 66506, USA*
⁶⁰*Louisiana Tech University, Ruston, Louisiana 71272, USA*
⁶¹*University of Maryland, College Park, Maryland 20742, USA*
⁶²*Boston University, Boston, Massachusetts 02215, USA*
⁶³*Northeastern University, Boston, Massachusetts 02115, USA*
⁶⁴*University of Michigan, Ann Arbor, Michigan 48109, USA*
⁶⁵*Michigan State University, East Lansing, Michigan 48824, USA*
⁶⁶*University of Mississippi, University, Mississippi 38677, USA*
⁶⁷*University of Nebraska, Lincoln, Nebraska 68588, USA*
⁶⁸*Princeton University, Princeton, New Jersey 08544, USA*
⁶⁹*State University of New York, Buffalo, New York 14260, USA*
⁷⁰*Columbia University, New York, New York 10027, USA*
⁷¹*University of Rochester, Rochester, New York 14627, USA*
- ⁷²*State University of New York, Stony Brook, New York 11794, USA*
⁷³*Brookhaven National Laboratory, Upton, New York 11973, USA*
⁷⁴*Langston University, Langston, Oklahoma 73050, USA*
⁷⁵*University of Oklahoma, Norman, Oklahoma 73019, USA*
⁷⁶*Oklahoma State University, Stillwater, Oklahoma 74078, USA*
⁷⁷*Brown University, Providence, Rhode Island 02912, USA*
⁷⁸*University of Texas, Arlington, Texas 76019, USA*
⁷⁹*Southern Methodist University, Dallas, Texas 75275, USA*
⁸⁰*Rice University, Houston, Texas 77005, USA*
- ⁸¹*University of Virginia, Charlottesville, Virginia 22901, USA*
⁸²*University of Washington, Seattle, Washington 98195, USA*

(Dated: April 16, 2007)

We describe a search for the standard model Higgs boson with a mass of $105 \text{ GeV}/c^2$ to $145 \text{ GeV}/c^2$ in data corresponding to an integrated luminosity of approximately 450 pb^{-1} collected with the D0 detector at the Fermilab Tevatron $p\bar{p}$ collider at a center-of-mass energy of 1.96 TeV . The Higgs boson is required to be produced in association with a Z boson, and the Z boson is required to decay to either electrons or muons with the Higgs boson decaying to a $b\bar{b}$ pair. The data are well

described by the expected background, leading to 95% confidence level cross section upper limits $\sigma(p\bar{p} \rightarrow ZH) \times B(H \rightarrow b\bar{b})$ in the range of 3.1 pb to 4.4 pb.

PACS numbers: 13.85.Ni, 13.85.Qk, 13.85Rm

Over the past two decades, increasingly precise experimental results have repeatedly validated the standard model (SM) and the relationship between gauge invariance and the embedded coupling strengths. For massive W and Z bosons, gauge invariance of the Lagrangian is preserved through the Higgs mechanism, but the Higgs boson (H) has yet to be observed. The current lower bound on the mass of the Higgs boson from direct experimental searches is $M_H = 114.4$ GeV/ c^2 at the 95% confidence level [1]. Searches for $p\bar{p} \rightarrow WH \rightarrow e(\mu)\nu b\bar{b}$, $p\bar{p} \rightarrow WH \rightarrow WWW^*$, and $p\bar{p} \rightarrow ZH \rightarrow \nu\bar{\nu} b\bar{b}$ have been recently reported [2–4]. The CDF collaboration has recently reported results in the $p\bar{p} \rightarrow WH \rightarrow \ell\nu$ channel [5] and previously reported results in the $p\bar{p} \rightarrow WH \rightarrow \ell\nu$ and $p\bar{p} \rightarrow ZH \rightarrow \ell^+\ell^- b\bar{b}$ ($\ell = e, \mu$) channels with significantly smaller data sets [6–8]. This Letter provides the first results from the D0 experiment of searches for a Higgs boson produced in association with a Z boson, which then decays either to an electron pair or to a muon pair. The Higgs is assumed to decay to a $b\bar{b}$ pair with a branching fraction given by the SM. The $Z(\rightarrow \ell^+\ell^-)H$ channels reported in this letter comprise major components of the search for a Higgs boson at the Tevatron collider.

Z bosons are reconstructed and identified through pairs of isolated electrons or muons with large momentum components transverse to the beam direction (p_T), having invariant mass consistent with that of the Z boson. Events are required to have exactly two jets identified as arising from b quarks (b jets). The resulting data are examined for the presence of a ($H \rightarrow b\bar{b}$) signal in the b -tagged dijet mass distribution. An efficient b -identification algorithm with low misidentification rate and good dijet mass resolution are essential to enhance signal relative to the backgrounds. The analysis of the dielectron [9] (dimuon [10]) channel is based on 450 ± 27 pb $^{-1}$ (370 ± 23 pb $^{-1}$) of data recorded by the D0 experiment between 2002 and 2004.

The D0 detector [11, 12] has a central-tracking system consisting of a silicon microstrip tracker (SMT) and a central fiber tracker (CFT), both located within a ≈ 2 T superconducting solenoidal magnet, with designs optimized for tracking and vertexing covering pseudorapidities $|\eta| < 3$ and $|\eta| < 2.5$, respectively ($\eta = -\ln[\tan(\theta/2)]$, with θ the polar angle relative to the direction of the proton beam). Central and forward preshower detectors are positioned just outside of the superconducting coil. A liquid-argon and uranium calorimeter has a central section (CC) covering pseudorapidities up to $|\eta| \approx 1.1$ and two end calorimeters (EC) that extend coverage to $|\eta| \approx 4.2$, with all three housed

in separate cryostats [12]. An outer muon system, covering $|\eta| < 2$, consists of a layer of tracking detectors and scintillation trigger counters in front of 1.8 T toroids, followed by two similar layers behind the toroids [13]. Luminosity is measured using plastic scintillator arrays placed in front of the EC cryostats [14].

The primary background to the Higgs signal is the associated production of a Z boson with jets arising from gluon radiation, among which $Z + b\bar{b}$ production is an irreducible background. The other background sources are $t\bar{t}$ production, diboson (ZZ and WZ) production, and events from multijet production that are misidentified as containing Z bosons. The backgrounds are grouped into two categories with the first category, called physics backgrounds, containing events with Z or W bosons arising from SM processes: inclusive $Z + b\bar{b}$ production, inclusive $Z + jj$ production in which j is a jet without b flavor, $t\bar{t}$, ZZ , and WZ events. This background is estimated from simulation as described below. The second category, called instrumental background, contains those events from multijet production that have two jets misidentified as isolated electrons or muons which appear to arise from the Z boson decay. This background is modeled using control data samples and the procedure described below.

Physics backgrounds are simulated using the leading order ALPGEN [15] and PYTHIA [16] event generators, with the leading order CTEQ5L [17] used as parton distribution functions. The decay and fragmentation of heavy flavor hadrons is done via EVTGEN [18]. The simulated events are passed through a detailed D0 detector simulation program based on GEANT [19] and are reconstructed using the same software program used to reconstruct the collider data. The ZH signal, for a range of Higgs masses, is also simulated using PYTHIA with the same processing as applied to data. Determination of the instrumental background and the normalization of the physics backgrounds are discussed below.

Candidate $Z \rightarrow ee$ events are selected using a combination of single-electron triggers. Accepted events must have two isolated electromagnetic (EM) clusters reconstructed offline in the calorimeter. Isolation is defined as $I = (E_{\text{total}}^{(0.4)} - E_{EM}^{(0.2)})/E_{EM}^{(0.2)}$ in which $E_{\text{total}}^{(0.4)}$ is the total calorimeter energy within $\Delta R < 0.4$ of the electron direction and $E_{EM}^{(0.2)}$ is the energy in the electromagnetic portion of the calorimeter within $\Delta R < 0.2$ of the electron direction. Candidate electrons must satisfy $I < 0.15$. Each EM cluster must have $p_T > 20$ GeV/ c and either $|\eta_{\text{det}}| < 1.1$ or $1.5 < |\eta_{\text{det}}| < 2.5$, where η_{det} is the pseudorapidity measured relative to the center of the detector, with at least one cluster satisfying $|\eta_{\text{det}}| < 1.1$.

In addition, the lateral and longitudinal shower shape of the energy cluster must be consistent with that expected of electrons. At least one of the two EM clusters is also required to have a reconstructed track matching the position of the EM cluster energy. Events with a dielectron mass of $75 < M_{ee} < 105$ GeV/ c^2 form the Z boson candidate sample in the dielectron channel.

Candidate $Z \rightarrow \mu^+ \mu^-$ events are selected using a set of single-muon triggers. Accepted events must have two isolated muons reconstructed offline. The muons must have opposite charge, $p_T > 15$ GeV/ c , and $|\eta| < 2.0$ with muon trajectories matched to tracks in the central tracking system (i.e., the SMT and the CFT), where the central track must contain at least one SMT measurement. In addition, the central tracks are required to have a distance of closest approach to the interaction vertex in the transverse plane smaller than 0.25 cm. Muon isolation is based on the sum of the energy measured in the calorimeter around the muon candidate and the sum of the p_T of tracks within $\Delta R = \sqrt{(\Delta\phi)^2 + (\Delta\eta)^2} = 0.5$ of the muon candidate normalized by the muon momentum. The distribution of this variable in background multi-hadron events is converted to a probability distribution such that a low probability corresponds to an isolated muon. The product of the probabilities for both muons in an event is computed, and the event is retained if the product is less than 0.02. Accepted Z boson candidates must have the opening angle of the dimuon system in the transverse plane (azimuth) of $\Delta\phi > 0.4$, and invariant mass 65 GeV/ $c^2 < M_{\mu\mu} < 115$ GeV/ c^2 . The $\Delta\phi$ requirement is used to protect against potential residual, difficult to model background from low mass dimuon production in which one of the muons is badly mismeasured. It is present in the preselection but has essentially no impact after the dimuon mass requirement. This mass range differs from that of the dielectrons because of the difference in resolutions of electron energies and muon momenta.

After selecting the Z candidate events, we define a Z +dijet sample which, in addition to satisfying the Z candidate selection requirements, has at least two jets in each event. Jets are reconstructed from energy in calorimeter towers using the Run II cone algorithm with $\Delta R = 0.5$ [20] with towers defined as non-overlapping, adjacent regions of the calorimeter $\Delta\eta \times \Delta\phi = 0.1 \times 0.1$ in size. The transverse momentum of each jet is corrected for multiple $p\bar{p}$ interactions, calorimeter noise, out-of-cone showering in the calorimeter, and energy response of the calorimeter as determined from the transverse momentum imbalance in photon+jet events [21]. Only jets that pass standard quality requirements and satisfy $p_T > 20$ GeV/ c and $|\eta| < 2.5$ are used in this analysis. The quality requirements are based on the pattern of energy deposition within a jet and consistency with the energy deposition measured by the trigger system.

For the $Z \rightarrow ee$ channel, the normalizations of the

smaller $t\bar{t}$, WZ and ZZ backgrounds are computed using simulated events and next-to-leading-order (NLO) cross sections. The cross sections were computed using the MCFM [22] program and the next-to-leading order CTEQ6M [23] parton distribution functions. Trigger efficiency, electron identification (ID) efficiency and resolution correction factors are derived from comparisons of data control samples and simulated events. The background contributions from $Z + jj$, $Z + bj$ and $Z + b\bar{b}$ processes are normalized to the observed Z +dijet data yield reduced by the expected contributions from the smaller physics and instrumental backgrounds. The relative fractions of the $Z + jj$, $Z + bj$ and $Z + b\bar{b}$ backgrounds in the Z +dijet sample are determined from the acceptance and selection efficiencies multiplied by the ratios of the NLO cross sections for these processes again computed using MCFM with CTEQ6M parton distribution functions. For the $Z \rightarrow \mu^+ \mu^-$ channel, all physics backgrounds are determined using simulated events with NLO cross sections again determined using MCFM and CTEQ6M. Trigger efficiency, muon ID efficiency, and resolution correction factors are derived from comparison of data control samples and the simulated events.

Instrumental backgrounds in both channels are determined by fitting the dilepton invariant mass distributions to a sum of non- Z and Z boson contributions. The Z boson lineshape is modeled using a Breit-Wigner distribution convoluted with a Gaussian representing detector resolution. The non- Z background, consisting of a sum of events from Drell-Yan production and instrumental background, is modeled using exponentials. The ratio of Z boson to non-resonant Drell-Yan production is fixed by the standard model.

The (two) jets arising from Higgs boson decay should contain b -flavored quarks, whereas background from Z +jets has relatively few events with b jets. To improve the signal-to-background ratio, two of the jets in the events from the Z +dijet sample are required to exhibit properties consistent with those of jets containing b quarks. The same b -jet identification algorithm [24] is used for the dielectron and dimuon samples. It is based on the finite lifetime of b hadrons giving a low probability that these tracks appear to arise from the primary vertex and considers all central tracks associated with a jet. A small probability corresponds to jets with tracks with large impact parameter, as expected in b hadron decays. The efficiency for tagging a b jet from Higgs decay is approximately 50%, determined as described in the next paragraph. The probability of misidentifying a jet arising from a charm quark as a b jet is roughly 20%. The inclusive Z +dijet sample has a $c\bar{c}$ content of roughly 2.3%. The probability to misidentify a jet arising from a light quark (u, d, s) or gluon as a b jet is roughly 4%. This choice of efficiency and purity optimizes the sensitivity of the analysis. The relatively large per-jet light-flavor misidentification rate can be accommodated because two

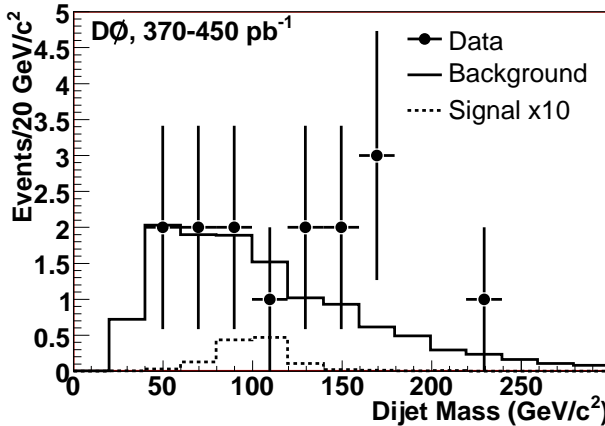


FIG. 1: The dijet invariant mass distribution in double-tagged Z +dijet events. The Higgs signal corresponds to $M_H = 115 \text{ GeV}/c^2$. (The uncertainties are statistical only.)

tagged jets are required in each event.

For background yields determined from simulated events, the probability as a function of jet p_T and η that a jet of a given flavor would be identified (tagged) as a b jet is applied to each jet in an event. The probability functions are derived from control data samples [25]. For jets in the simulated events, the flavor is determined from a priori knowledge of the parton that gives rise to the jet. The probability of having two b -tagged jets is defined by convoluting the per-jet probabilities assuming there are no jet-to-jet correlations introduced by the b -tag requirement. The observed number of $Z+2$ b -jet events and the predicted background levels are shown in Table I.

The invariant mass of the two b jets in the $Z+2$ b jet sample is shown in Fig. 1. This distribution is searched for an excess of events. The peak position in the dijet mass spectrum is expected to be at a lower value than the hypothetical Higgs mass because the jet energy is corrected to reflect the energy of particles in the jet cone without a general correction for the lower b jet response compared with light jets. If any good muon is within $\Delta R < 0.5$ of the jet, then twice the muon momentum is added to the jet momentum (after applying the standard jet correction). This is an approximation to the energy of both the muon and the accompanying neutrino. The expected contribution from Higgs boson production shown in Fig. 1 corresponds to $M_H = 115 \text{ GeV}/c^2$.

Systematic uncertainties for signal and background arise from a variety of sources, including uncertainties on the trigger efficiency, on the corrections for differences between data and simulation for lepton reconstruction and identification efficiencies, lepton energy resolution, jet reconstruction efficiencies and energy determination, b -identification efficiency, uncertainties from theory and parton distribution functions for cross sections used for simulated events and uncertainties on the method used

for instrumental background estimates. The luminosity measurement has an uncertainty of 6.1%. This uncertainty is applied as systematic uncertainty to the background predictions which are absolutely normalized using simulation and to the luminosity input to the limit calculation. The uncertainties from these sources are shown in Table II. These are evaluated by varying each of the corrections by $\pm 1\sigma$, by comparing different methods (for the instrumental backgrounds), and by varying the parton distribution functions among the 20 error sets provided as part of the CTEQ6L library. The variations seen for different processes for a given uncertainty arise because of differences among the various background processes and because of intrinsic differences in the kinematic spectra from different Higgs mass hypotheses.

The observed yield is consistent with background predictions. Upper limits on the ZH production cross section are derived at 95% confidence level using the CL_s method [26], a modified frequentist procedure, with a log-likelihood ratio classifier. The shapes of full dijet invariant-mass spectra of the signal and background histogrammed in 5 GeV/c^2 bins are used to produce likelihoods that the data are consistent with the background-only hypothesis or with a background plus signal hypothesis. Systematic uncertainties are folded into the likelihoods via Gaussian distribution, with correlations maintained throughout. The data yield, predicted backgrounds and expected and observed limits are shown in Table III for five hypothetical Higgs masses. The limits are also shown in Fig. 2. The mass window in Table III is used for illustration. It is centered on the mean of the reconstructed Higgs mass in simulated ZH events and has a width of $\pm 1.5\sigma$ in which σ is the result of a Gaussian fit to the reconstructed dijet mass distribution. The upper bounds differ slightly between the $Z \rightarrow ee$ and $Z \rightarrow \mu^+\mu^-$ events because of different resolutions.

In summary, we have carried out a search for associated ZH production in events having two high- p_T electrons or muons and two jets identified as arising from b quarks. Consistency is found between data and background predictions. A 95% confidence level upper limit on the Higgs boson cross section $\sigma(p\bar{p} \rightarrow ZH) \times B(H \rightarrow b\bar{b})$ is set between 4.4 pb and 3.1 pb for Higgs bosons with mass between 105 GeV/c^2 and 145 GeV/c^2 , respectively.

We thank the staffs at Fermilab and collaborating institutions, and acknowledge support from the DOE and NSF (USA); CEA and CNRS/IN2P3 (France); FASI, Rosatom and RFBR (Russia); CAPES, CNPq, FAPERJ, FAPESP and FUNDUNESP (Brazil); DAE and DST (India); Colciencias (Colombia); CONACyT (Mexico); KRF and KOSEF (Korea); CONICET and UBACyT (Argentina); FOM (The Netherlands); PPARC (United Kingdom); MSMT and GACR (Czech Republic); CRC Program, CFI, NSERC and WestGrid Project (Canada); BMBF and DFG (Germany); SFI (Ireland); The Swedish Research Council (Sweden); CAS and CNSF (China);

TABLE I: Number of observed and expected background events.

Final state	$Z + \geq 2 \text{ jets}$			$2 b \text{ tags}$		
	$Z \rightarrow ee$	$Z \rightarrow \mu^+ \mu^-$	$Z \rightarrow \ell^+ \ell^-$	$Z \rightarrow ee$	$Z \rightarrow \mu^+ \mu^-$	$Z \rightarrow \ell^+ \ell^-$
Zbb	9.4	8.3	17.4	2.0	1.3	3.3
Zjj	414	437	851	1.2	2.6	3.8
$t\bar{t}$	2.7	9.6	12.3	0.83	3.1	3.9
$ZZ + WZ$	9.2	21.4	30.6	0.32	0.42	0.74
Instrumental	28.0	16.1	44.1	0.18	0.41	0.59
Total background	463	493	956	4.5	7.8	12.3
Observed events	463	545	1008	5	10	15

TABLE II: Systematic uncertainty in background and signal predictions given as the fractional uncertainty on the event totals. The ranges correspond to variations introduced by different processes (background), the dijet mass window requirement (background and signal) and intrinsic differences in kinematics arising from different hypothesized Higgs masses (signal).

Source	Background	Signal
Lepton ID Efficiencies	11% – 16%	11% – 12%
Lepton Resolution	2%	2%
Jet ID Efficiency	5% – 11%	8%
Jet Energy Reconstruction	10%	7%
b -jet ID Efficiency	10% – 12%	9%
Cross Sections	6% – 19%	7%
Trigger Efficiency	1%	1%
Luminosity	3%	6.1%
Instrumental Background	2% (ee) 12% ($\mu\mu$)	

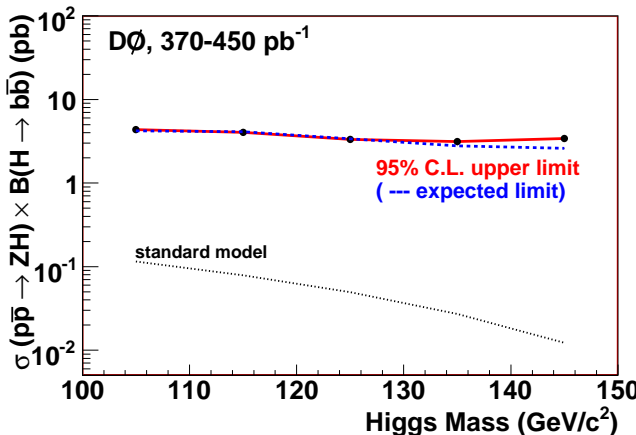


FIG. 2: The expected and observed cross-section limits are shown as a function of Higgs mass. The cross section based on the SM is shown for comparison.

Alexander von Humboldt Foundation; and the Marie Curie Program.

- [*] Visitor from Augustana College, Sioux Falls, SD, USA.
- [¶] Visitor from The University of Liverpool, Liverpool, UK.
- [§] Visitor from ICN-UNAM, Mexico City, Mexico.
- [‡] Visitor from Helsinki Institute of Physics, Helsinki, Finland.
- [#] Visitor from Universität Zürich, Zürich, Switzerland.
- [1] The ALEPH, DELPHI, L3 and OPAL Collaborations, Phys. Lett. B **565**, 61 (2003).
- [2] V.M. Abazov, et al. (D0 Collaboration), Phys. Rev. Lett. **94**, 091802 (2005).
- [3] V.M. Abazov, et al. (D0 Collaboration), Phys. Rev. Lett. **97**, 151804 (2006).
- [4] V.M. Abazov, et al. (D0 Collaboration), Phys. Rev. Lett. **97**, 161803 (2006).
- [5] A. Abulencia et al. (CDF Collaboration), Phys. Rev. Lett. **96**, 081803 (2006).
- [6] F. Abe et al. (CDF Collaboration), Phys. Rev. Lett. **79**, 3819 (1997).
- [7] F. Abe et al. (CDF Collaboration), Phys. Rev. Lett. **81**, 5748 (1998).
- [8] D. Acosta et al. (CDF Collaboration), Phys. Rev. Lett. **95**, 051801 (2005).
- [9] J.M. Heinmiller, Ph.D. Dissertation, University of Illinois at Chicago, FERMILAB-THESIS-2006-30 (2006).
- [10] H. Dong, Ph.D. Dissertation, Stony Brook University, FERMILAB-THESIS-2007-11 (2007).
- [11] V.M. Abazov, et al. (D0 Collaboration), Nucl. Instrum. and Methods A **565**, 463 (2006).
- [12] S. Abachi et al. (D0 Collaboration), Nucl. Instrum. Methods A **338**, 185 (1994).
- [13] V.M. Abazov et al. (D0 Collaboration), Nucl. Instrum. and Methods A **552**, 372 (2005).
- [14] T. Andeen et al., FERMILAB-TM-2365-E (2006), in preparation.
- [15] M.L. Mangano, M. Moretti, F. Piccinini, R. Pittau, and A. Polosa, J. High Energy Phys. **07**, 001 (2003).
- [16] T. Sjöstrand et al., Comput. Phys. Commun. **135**, 238 (2001).
- [17] H.L. Lai et al., Phys. Rev. D **55**, 1280 (1997).
- [18] D.J. Lange, Nucl. Instrum. and Methods A **462**, 152 (2001).
- [19] R. Brun and F. Carminati, CERN Program Library Long Writeup W5013 (1993).
- [20] G.C. Blazey et al., hep-ex/0005012.
- [21] V.M. Abazov et al. (D0 Collaboration), Phys. Rev. D **74**, 092005 (2006).

TABLE III: Numbers of predicted background and signal events and the observed yield after all selection requirements, including the addition of a dijet mass window. The window is applied for illustration, showing the yields in the region of highest predicted signal-to-background ratio. Also shown are the expected and observed upper limits on the cross section for each channel and for the combined analysis at 95% confidence level computed as described in the text.

	$M_H = 105 \text{ GeV}/c^2$		$M_H = 115 \text{ GeV}/c^2$		$M_H = 125 \text{ GeV}/c^2$	
	ee	$\mu\mu$	ee	$\mu\mu$	ee	$\mu\mu$
Mass window(GeV/c^2)	[65, 113]	[65, 118]	[72, 125]	[70, 128]	[75, 136]	[78, 137]
Predicted signal	0.08	0.06	0.06	0.05	0.05	0.03
Background	1.6	3.1	1.7	3.1	1.8	2.8
Data	2	3	1	3	1	4
Expected σ_{95}	5.6	9.9	5.7	8.6	4.5	7.7
Observed σ_{95}	5.4	11.1	4.9	10.5	3.6	11.0
Expected σ_{95}	4.2 pb		4.1 pb		3.4 pb	
Observed σ_{95}	4.4 pb		4.0 pb		3.3 pb	

	$M_H = 135 \text{ GeV}/c^2$		$M_H = 145 \text{ GeV}/c^2$	
	ee	$\mu\mu$	ee	$\mu\mu$
Mass window(GeV/c^2)	[82, 143]	[84, 147]	[87, 156]	[92, 160]
Predicted signal	0.027	0.022	0.015	0.01
Background	1.6	2.9	1.6	2.8
Data	1	5	0	6
Expected σ_{95}	4.0	5.5	3.1	7.1
Observed σ_{95}	3.1	9.3	2.5	13.7
Expected σ_{95}	2.8 pb		2.6 pb	
Observed σ_{95}	3.1 pb		3.4 pb	

- [22] J. Campbell and K. Ellis, <http://mcfm.fnal.gov/>
- [23] J. Pumplin *et al.*, J. High Energy Phys. **0207**, 12 (2002).
- [24] S. Greder, Ph.D. dissertation, Université Louis Pasteur, Strasbourg, FERMILAB-THESIS-2004-28.
- [25] B. Clement, Ph.D. dissertation, Strasbourg, IReS, FERMILAB-THESIS-2006-06.
- [26] T. Junk, Nucl. Instrum. Methods A **434**, 435 (1999), A. Read, proceedings of the “1st workshop on Confidence Limits”, edited by F. James, Y. Perrin and L. Lyons, CERN-2000-005.